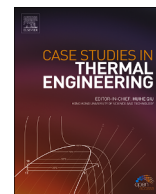




Contents lists available at ScienceDirect

Case Studies in Thermal Engineering

journal homepage: www.elsevier.com/locate/csite

Comprehensive characterization and kinetic analysis of coconut shell thermal degradation: Energy potential evaluated via the Coats-Redfern method

Minhaj Uddin Monir^{b, c}, Shaik Muntasir Shovon^{b, c}, Faysal Ahamed Akash^{b, c},
Md Ahasan Habib^d, Kuaanan Techato^a, Azrina Abd Aziz^e,
Shahariar Chowdhury^{a, f, g, *}, Tofan Agung Eka Prasetya^{h, **}

^a Faculty of Environmental Management, Prince of Songkla University, Songkhla, 90112, Thailand

^b Department of Petroleum and Mining Engineering, Jashore University of Science and Technology, Jashore, 7408, Bangladesh

^c Energy Conversion Laboratory, Department of Petroleum and Mining Engineering, Jashore University of Science and Technology, Jashore, 7408, Bangladesh

^d Geological Survey of Bangladesh, Pioneer Road, Segunbagicha, Dhaka, 1000, Bangladesh

^e Faculty of Civil Engineering Technology, Universiti Malaysia Pahang Al-Sultan Abdullah, 26300 Gambang, Kuantan, Pahang, Malaysia

^f Health and Environmental Research Center, Faculty of Environmental Management, Prince of Songkla University, HatYai, 90110, Songkhla, Thailand

^g Faculty of Health and Life Sciences, INTI International University Persiaran Perdana BBN, Putr Nilai, 71800, Nilai, Negeri Sembila, Malaysia

^h Department of Health, Faculty of Vocational Studies, Universitas Airlangga, Surabaya, 60285, East Java, Indonesia

ARTICLE INFO

Keywords:

Kinetic analysis
Coats-Redfern method
Coconut shell pyrolysis
Thermodynamic characteristics
Activation energy

ABSTRACT

Coconut shell represents a promising biomass for energy production, given their wide availability. In this study, the thermo-kinetics of coconut shells were examined through thermogravimetric analysis from 30 °C to 1000 °C at 5 °C/min under N₂. Advanced analytical tools assessed the elemental, microstructural, and morphological attributes of the samples. The thermal degradation unveiled three phases: dehydration, devolatilization, and combustion. Notably, the Coats-Redfern method detailed the devolatilization stage, pinpointing the coconut shell's thermal and kinetic attributes. The Zhuravlev diffusion equation (DM6) emerged as the most suitable model, with an activation energy (E_a) and pre-exponential factor of 68.9 kJ mol⁻¹ and 0.05 min⁻¹, respectively. Thermodynamic values such as enthalpy (ΔH), Gibbs free energy (ΔG), and entropy (ΔS) for devolatilization were 65.2, 193.1, and -0.28117, respectively. Collectively, the findings underscore the significant bioenergy potential of coconut shells, positioning them as a sustainable alternative to traditional energy. Such insights play a crucial role in improving pyrolysis reactor designs and comprehending the mechanisms of coconut shell pyrolysis, offering potential solutions for energy deficits and environmental concerns.

1. Introduction

Conventional fossil fuels-coal, oil, and natural gas-currently dominate global energy production, catering to approximately 84% of the world's energy consumption [1,2]. In contrast, renewable energy sources, including hydro, wind, and solar, fulfill the remaining demand [3]. Although the International Energy Agency (IEA) noted a 4% decline in global energy demand in 2020 due to the COVID-

* Corresponding author. Faculty of Environmental Management, Prince of Songkla University, Songkhla 90112, Thailand.

** Corrospoding author. Faculty of Vocational Studies, Universitas Airlangga, Surabaya, 60285, East Java, Indonesia.

E-mail addresses: Mdshahariar.c@psu.ac.th (S. Chowdhury), tofana-agung-e-p@vokasi.unair.ac.id (T.A. Eka Prasetya).

<https://doi.org/10.1016/j.csite.2024.104186>

Received 14 October 2023; Received in revised form 6 January 2024; Accepted 26 February 2024

Available online 27 February 2024

2214-157X/© 2024 The Authors. Published by Elsevier Ltd. This is an open access article under the CC BY-NC license (<http://creativecommons.org/licenses/by-nc/4.0/>).

19 pandemic, this rebounded in 2021, with expectations of continuous growth in subsequent years [4,5]. While fossil fuels persist as the major energy providers, sustainable energy's evolution is palpably gaining momentum and is anticipated to significantly influence future energy landscapes [6]. Particularly, coal accounts for about 37% of global electricity production [7], but its usage is waning due to environmental and health concerns. Natural gas, deemed a transitional fuel, has witnessed rapid adoption, with forecasts suggesting a 30% rise in consumption by 2040 [8]. Despite renewables constituting 72% of newly added power capacity in 2020, they still form a minor fraction of the total energy mix, necessitating substantial investments for wider deployment [9,10]. However, the growth of electric vehicles and sustainable energy is expected to reduce the consumption of fossil fuels for energy generation in the coming decades. Natural gas has emerged as the fastest-growing fossil fuel, and projections indicate that its consumption will experience a significant uptick of around 30% by the year 2040 [11]. It is often seen as a transition fuel to help countries move away from coal towards cleaner energy sources. Renewable energy is growing rapidly, with solar and wind power leading the way. Global statistics for 2020 revealed that renewable energy accounted for nearly 72% of newly added power capacity across the world [12,13]. However, renewable energy source is still accounted for a relatively small portion of total energy consumption, and significant investment is needed to accelerate their deployment [14]. Ali, Bahaitham and Naebulharam [15] investigated coconut shell utilizing both model-free and model-fitting methods, determining an activation energy range of 79.1–226.5 kJ mol⁻¹. Moreover, Cheng, Ding, Guo, He, Gong, Alexander and Yu [16] conducted a study on the hydrothermal carbonization and kinetic modeling of coconut shell. In the work by da Silva, Alves, de Araujo Galdino, de Sena and Andersen [17], coconut shell was analyzed using model-free methods, revealing a higher heating value of 18.64 MJ kg⁻¹.

Coconut shell emerges as a sustainable biomass resource with notable potential for biofuel production and value-added byproducts like biochar [18,19]. Thermal decomposition kinetics offer a promising avenue to transform coconut shells into bioenergy. These byproducts have diverse applications, ranging from soil improvement to water treatment and energy generation [20]. While implementing varied heating rates in kinetic studies refines the activation energy estimation (E_a) and enhances the model's alignment with experimental outcomes [21], it is noteworthy that no other researcher in Bangladesh has previously identified the activation energy, frequency factor, entropy, Gibbs free energy, or entropy of coconut shell. A potential research gap in the study of coconut shell thermal degradation lies in the limited exploration of the influence of varying process parameters on the kinetics of degradation, hindering a comprehensive understanding essential for optimizing energy potential through the Coats-Redfern method. Therefore, this research delves into the comprehensive thermal breakdown of the coconut shell, emphasizing its thermal, devolatilization, kinetic, pyrolytic, and thermodynamic aspects using the Coats-Redfern approach. Applying sophisticated methods such as scanning electron microscopy (SEM), field emission scanning electron microscopy (FE-SEM) coupled with energy-dispersive X-ray spectroscopy (EDX), fourier transform infrared spectroscopy (FTIR), and thermogravimetric analysis (TGA), this research aims to attain a comprehensive understanding of the properties and behavior of coconut shells. Our objective is to decipher the intrinsic mechanisms steering the thermal decomposition kinetics of the coconut shell, assessing its viability as a green energy resource. The insights gleaned hold profound implications for promoting sustainable technologies that valorize coconut shells and comparable biomass resources. The outcome of this study will contribute significantly to the scientific community in Bangladesh by enhancing our understanding of its potential applications in various industries.

2. Materials and method

2.1. Sampling collection and processing

Three samples of coconut shells were collected from a local farm at Islampur in Jashore, Bangladesh, as depicted in Fig. 1. To eliminate potential contaminants, an initial cleaning procedure was executed using compressed gas, followed by a subsequent rinse with distilled water. Based on methodologies referenced in Refs. [22,23], the shells were subjected to heating at a constant temperature of 110 °C until a weight equilibrium was observed. For granulometric standardization, the shells were initially processed to a micron scale using laboratory-grade shredders. This was supplemented with an additional comminution step using crushers. The final material was then sieved to ensure a consistent particle size, using a sieve plate with apertures of 130 μm.

2.2. Characterization

By maintaining the American Society for Testing and Materials (ASTM) standard methods, thermal analysis was conducted using an electric oven and muffle furnace. This study was done to mark the amount of moisture content, volatile matter, fixed carbon, and ash content in the samples. Ultimate study was conducted using a CHNS elemental analyzer (PerkinElmer 2400II, USA). The higher heating value (HHV) measurement was conducted using a 1341 Plain Jacket Calorimeter, which was calibrated prior to experimentation. The procedure adhered to ASTM E711 guidelines, and to ensure the accuracy of the results, the tests were carried out in triplicate. To recognize the functional groups that exist in coconut shell, a PerkinElmer spectrum FT-IR Spectrometer was used. In this research, SEM analysis (Brand: Fei, Model: Quanta 450) was employed to examine the morphological characteristics of coconut shells. High-resolution images and elemental composition data were acquired through FESEM-EDX analysis (Brand: Jeol, Model: JSM-7800F). The morphology of the coconut shell was assessed using FESEM-EDX spectra obtained with a SIRION200 Schottky field emission scanning electron microscope (SFE-SEM), which was equipped with a Rontec EDX system.

2.3. Thermogravimetric analysis

For analyzing the thermal degradation characteristics of the coconut shell, TGA was conducted using a (Q 500 series) TGA instrument (TA Instruments, USA). The TGA was performed on the sample, weighing between 10 ± 0.5 mg. The study involved determining the mass loss of the coconut shell while it was heated from 30 °C to 1000 °C at 5 °C/min heating rate. To maintain an inert atmos-

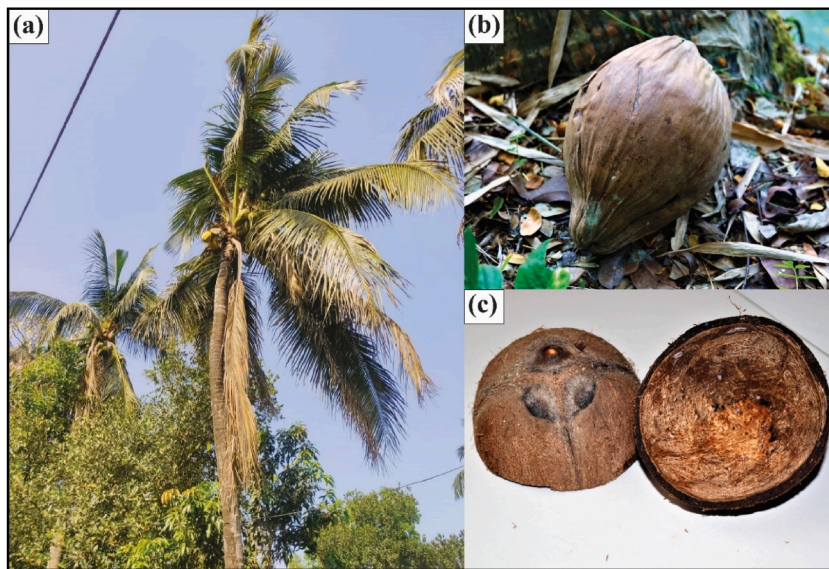


Fig. 1. Samples collection and preparation: (a) coconut tree and (b, c) coconut shell separated and ready for drying under the sun.

where, nitrogen gas was used with a 60 mL/min flow rate. The TGA was repeated three times using the same heating rate to achieve the highest accuracy with the lowest error. In addition to understanding the thermal breakdown behavior during pyrolysis process and calculating the kinetics and thermodynamic characteristics of the process, the TGA data were used.

2.4. Kinetic study

2.4.1. The equation for the Coats-Redfern model

Chemical processes involve rearranging the molecular or ionic components of a reactant to another products [24]. In the case of biomass conversion, the reactant is often a solid substance made of a range of organic compounds, and the yield of the reaction is indicated by the production of non-condensable gases, bio-oil, and biochar. The level of conversion may be used to determine how far a reaction has proceeded. This can be measured for pyrolysis or combustion processes by analyzing the changes in heat (using calorimetry) or mass (using thermogravimetry). The amount of conversion may be stated mathematically (Eq. (1)) as-

$$\alpha = \frac{x_{initial} - x_t}{x_{initial} - x_{final}} \dots \dots \dots (1)$$

Where, $x_{initial}$ = initial value, x_{final} = final value, x_t = value at time t, α = extent of conversion.

Temperature (T), pressure (p), and the degree of conversion (α) all affect the kinetics of a chemical reaction, which is defined as the rate of change in the amount of conversion over time. As a result, the rate equation can be represented mathematically by a function that incorporates all of these components.

$$\frac{d\alpha}{dt} = k(T)f(\alpha)h(p) \dots \dots \dots (2)$$

where, h (p) is ignored in most kinetic computations for thermal decomposition [25]. Eq. (2) then can be truncated as-

$$\frac{d\alpha}{dt} = k(T)f(\alpha) \dots \dots \dots (3)$$

It is essential to remember that the influence of pressure on a reaction cannot be underestimated, particularly in processes involving gaseous reactants or products. The rate of conversion is likewise temperature dependent and is typically denoted by the "rate constant" k(T). It is not, however, a constant and can be expressed using the Arrhenius equation.

$$K(T) = A e^{-\frac{E_a}{RT}} \dots \dots \dots (4)$$

Where, A = pre-exponential factor, min^{-1} , E_a = Activation energy, KJ.mol^{-1} , R = Universal gas constant, T = Absolute temperature.

The E_a of a reactant can be regarded as the lowest energy required to stimulate the reactants to reach an active state, where a reaction can occur. The reaction environment provides the energy needed to break the necessary bonds and make an active or transition-state complex, which then moves on to the next step of the reaction [26]. The pre exponential factor (A), also referred to as the "fre-

quency factor" or "attempted frequency," can be expressed as the number of collisions per unit time that occur with the appropriate orientation to react [27].

Combination of Eq. (3) and Eq. (4) generate Eq. (5) is as follows-

$$\frac{d\alpha}{dt} = A e^{-\frac{E}{RT}} f(\alpha) \dots\dots\dots (5)$$

The function f(α) signifies the liaison between the conversion rate and the extent of conversion and can be denoted as the reaction model. During the course of kinetic calculations, it is common to encounter the integral form of a reaction model expressed as g (α) in Eq. (6).

$$g(\alpha) = \int_0^\alpha \frac{d\alpha}{f(\alpha)} = A \int_0^t e^{-\frac{E}{RT}} dt \dots\dots\dots (6)$$

From Eq. (6), it can be inferred that by knowing A, E, and f (α), the conversion rate can be explicitly expressed. The appropriate amalgamation of kinetic factors A, E, and f(α) is referred to as the "kinetic triplet," which describes a specific reaction. The primary goal of kinetic analysis is to determine the kinetic triplet, which includes the E_a, A, and reaction order.

Eq. (6) can be modified at a heating rate β, such that β = $\frac{dT}{dt}$.

$$\begin{aligned} g(\alpha) &= \int_0^\alpha \frac{d(\alpha)}{f(\alpha)} \\ &= \frac{A}{\beta} \int_{T_0}^{T_\alpha} e^{-\frac{E}{RT}} dT \\ &= \frac{A}{\beta} \int_0^{T_\alpha} e^{-\frac{E}{RT}} dT \\ &= \frac{AE}{\beta R} p(x) \dots\dots\dots (7) \end{aligned}$$

$$\text{Or, } g(\alpha) = \frac{AE}{\beta R} \int_x^\infty \frac{e^{-x}}{x^2} dx \dots\dots\dots (8)$$

Where, $x = \frac{E}{RT}$ and $p(x) = \int_x^\infty \frac{e^{-x}}{x^2} dx$.

The reason for substituting the lower limit of temperature integral in Eq. (7) with 0 instead of T₀ is that there is no chemical reaction that takes place within the temperature range of 0 to T₀. This substitution can be acceptable by considering the statistic that the reaction rate is directly proportional to temperature and is negligible at temperatures close to absolute zero. Therefore, any contribution to the integral from the temperature range of 0 to T₀ is negligible and can be safely ignored.

Due to the inability to derive an analytical solution for the integral term present on the right-hand side of Eq. (8), Coats and Redfern resorted to the application of the Rainville function as a means of obtaining a solution. As a result of this approach, they derived the Coats-Redfern equation [28] which can be written in a mathematical formula as (Eq. (9)):

$$\ln \left[\frac{g(\alpha)}{T^2} \right] = \ln \left[\left(\frac{AR}{\beta E} \right) \left(1 - \frac{2RT}{E} \right) \right] - \frac{E_a}{RT} \dots\dots\dots (9)$$

Activation energy (E_a) and frequency factor (A) was computed by plotting a curve from Eq. (9) in $[\frac{g(\alpha)}{T^2}]$ vs 1000/T(K). The E_a can be computed using the slope of the straight line, (-E/R) and $\ln(\frac{AR}{\beta E})$ will be its intercept. The suitable reaction mechanism approach g (α) was applied to determine the values of E_a and A. The values of these parameters were obtained by estimating the slope and intercepting the regression lines. Twenty-one reaction mechanism models (Table 1) were included in this study to determine the kinetic and thermodynamic parameters for coconut shell.

2.4.2. Thermodynamic data calculation

In order to calculate the thermodynamic characteristics (ΔH, ΔG, and ΔS), related to kinetics data were used. The relations utilized to calculate thermodynamic characteristics are shown from Eqs. (10)–(12).

$$\text{Enthalpy Change } \Delta H = E_a - R \times T \dots\dots\dots (10)$$

$$\text{Gibbs free energy } \Delta G = E_a + R \times T_m \times \ln(K_b \times T/h \times A) \dots\dots\dots (11)$$

$$\text{Entropy } \Delta S = (\Delta H - \Delta G)/ T_m \dots\dots\dots (12)$$

Table 1
Function $g(\alpha)$ as a Representation of Reaction Mechanism Models in the Coats-Redfern Method.

Model Name	Symbol	$g(\alpha)$
0 th Order	CRO0	α
1st Order	CRO1	$-\ln(1-\alpha)$
1.5th	CRO1.5	$2[(1-\alpha)^{-1.5}-1]$
2nd Order	CRO2	$[1/(1-\alpha)]-1$
3rd Order	CRO3	$0.5[(1-\alpha)^{-2}-1]$
1 way Transport	DM1	α^2
2 way Transport	DM2	$(1-\alpha)-\ln(1-\alpha)+\alpha$
3 way Transport	DM3	$[-\ln(1-\alpha)]^{1/3}^2$
Valensi equation	DM4	$\alpha+(1-\alpha)\ln(1-\alpha)$
Ginstling Brounstein equation	DM5	$(1-2\alpha/3)\cdot(1-\alpha)^{2/3}$
Zhuravlev equation	DM6	$[(1-\alpha)^{-1/3}-1]^2$
Jander equation	DM7	$[1-(1-\alpha)^{1/3}]^2$
Ginstling equation	DM8	$1-(0.67\alpha)-(1-\alpha)^{0.67}$
Cylindrical Shape	GM1	$1-(1-\alpha)^{1/2}$
Sphere Shape	GM2	$1-(1-\alpha)^{1/3}$
1/2 power law	NM1	$\alpha^{1/2}$
1/3 power law	NM2	$\alpha^{1/3}$
1/4 power law	NM3	$\alpha^{1/4}$
1/2 Avrami Erofeev Equation	NM4	$[-\ln(1-\alpha)]^{1/2}$
1/3 Avrami Erofeev Equation	NM5	$[-\ln(1-\alpha)]^{1/3}$
2/3 Avrami Erofeev Equation	NM6	$[-\ln(1-\alpha)]^{2/3}$

3. Result and discussion

3.1. Coconut shell characterization

Table 2 represents the proximate and ultimate results of coconut shell, with coal and other coconut shell values provided as a reference. The examined results (mean \pm SD) of samples ash yield 6.7 ± 0.05 %, volatile matter 49.9 ± 0.48 %, fixed carbon 36.5 ± 0.35 %, and moisture 6.9 ± 0.07 %, respectively. Compared to bituminous coal, coconut shell shows high volatile matter (mean, 49.9 ± 0.48 %) and low level of ash content (6.7 ± 0.05 %) indicating coconut shell appropriate for thermal applications and prospecting a higher amount of bio-oil production. In addition, the investigated coconut shells make them a better ignition fuel and results in less slagging, low contamination, and poor agglomeration. Moreover, with a low ash content in biomass incurs negligible processing and least management cost [29]. While selecting a fuel, the percentage of moisture content is another crucial consideration [30]. In that case, with a <10 wt% of moisture content biomass can be a suitable feedstock. The fixed content of carbon in coconut shell is 36.5 ± 0.35 wt%, significantly less than coal. Fixed carbon is the remaining combustible product after the devolatilization region that gives the information of the extent of pyrolysis kinetics throughout thermochemical processes [31]. Due to the lower amount of sulfur (0.5 ± 0.01 %) and nitrogen (2.1 ± 0.01 %) content in coconut shells, the mixture of NO_x and SO_x throughout pyrolysis process will be negligible. Coconut shells contain a significant volume of fixed carbon ($41.8 \pm$ wt.%) and hydrogen ($4.1 \pm$ wt.%), that indicates their potential as a fuel source.

Higher heating value (HHV), indicative of potential energy output of a fuel, is determined to quantify the energy that was released from a fuel when it is completely combusted. It is defined as the amount of heat energy that is released when one unit of mass of fuel is completely burned. This includes the energy that is released when any water vapour that forms during the burning process turns into liquid water. Fig. 2 shows the HHV of coconut shell and other biomass components. From the figure it is clear that coconut shell has a HHV of 17400 (KJ kg⁻¹) compared to other sources.

Table 2
Proximate and ultimate analyses of coconut shell samples (n = 3), mean \pm SD and compared with others.

Analysis	Current/This study	Coconut shell ^a	Bituminous coal ^b
Proximate analysis (dry basis wt.%)			
Ash content	6.7 ± 0.05	5.2	12.9
Volatile material	49.9 ± 0.48	71.7	21.8
Fixed carbon	36.5 ± 0.35	11.8	57.9
Moisture content	6.9 ± 0.07	8.3	7.4
Ultimate analysis (dry basis wt.%)			
C	41.8 ± 0.65	42.3	66.5
O	51.5 ± 0.51	52.0	13.3
H	4.1 ± 0.08	4.6	4.4
S	0.5 ± 0.01	0.4	0.6
N	2.1 ± 0.01	0.6	1.2

^a Menon, Sampath and Kaarthik [32].

^b Coppola, Solimene, Bareschino and Salatino [33].

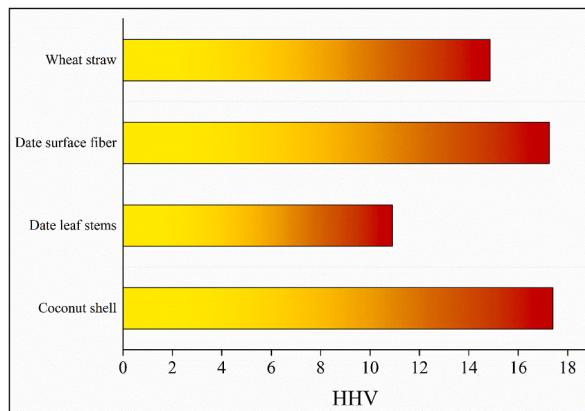


Fig. 2. HHV (KJ.kg⁻¹) of coconut shell and other biomass components [34].

In Fig. 3a, SEM image provides valuable insights into the surface morphology of the coconut shell sample under investigation. A closer analysis of the microstructure indicates that the particles exhibit a notable degree of variation in terms of their size and shape. The coconut shell particles can be separated into distinct classes based on the aforementioned observations. These categories include large fibrous particles with an average length of 92.0 μm (range: 112.4 to 38.3 μm) and width of 15.4 μm (range: 26.4 to 9.3 μm). Irregular spherical or prismatic porous particles are observed. The FESEM photomicrograph (Fig. 3b) provides a detailed view of the fibrous particles, revealing their surfaces rough, irregular spherical or semispherical lens-like morphological structures. The average diameter of these lenses is 1.9 μm . The sample contains a significant proportion of carbon (56.1%), and oxygen (42.6%), as well as smaller quantities of zinc (0.22%), phosphorous (0.62%), and sulfur (0.31%). Nitrogen and trace elements are presented in the sample.

FTIR spectra from Fig. 4, shows that coconut shell is a lignocellulosic product which is mostly formed of cellulose, lignin, and hemicellulose. As a result, it contains various oxygenated functional groups such as esters, ketones, alkanes, aromatics, and alcohols [35]. The absorption groups observed at 3444 cm^{-1} correspond to the O–H stretching [36]. Coconut shell, on the other hand, has additional bands at 2912 cm^{-1} due to C–H stretching [37]. Moreover, two significant bands at 1262 cm^{-1} and 1045 cm^{-1} are detected in coconut shell, that indicate CH₂ symmetric stretching [38]. Additional minor group detected at 617 cm^{-1} was related with C–O–C stretching which consistent with other [38]. The spectra of the sample also reveals the presence of bands related with cellulose, hemi-

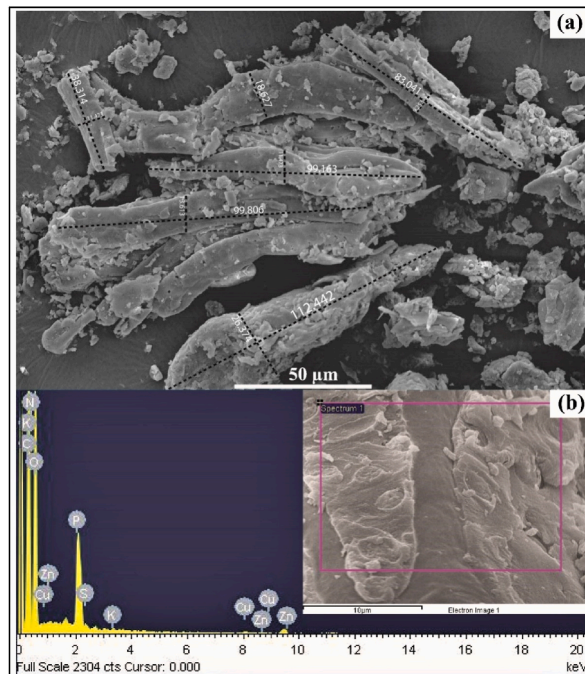


Fig. 3. Morphological characteristics of coconut shell: (a) SEM image (b) FESEM with EDX.

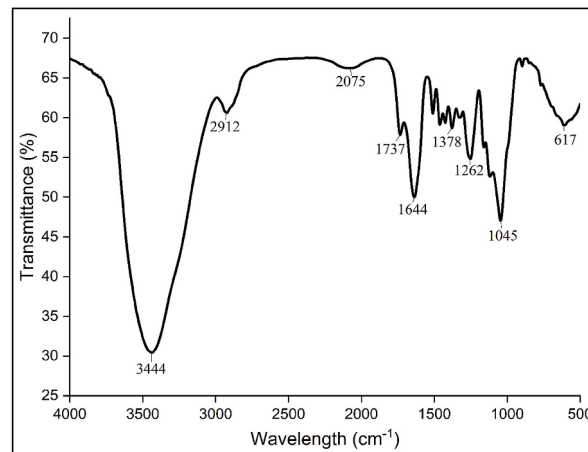


Fig. 4. FT-IR spectrum for coconut shell.

cellulose, or lignin, which was consistent with reference [39]. Based on the results, it is likely the results indicate that the investigated coconut shell contains C-H, O-H, and CH₂ stretching.

3.2. Thermal degradation characteristics and behavior of coconut shell

Coconut shells are mainly characterized by hemicellulose, cellulose, and lignin. Every element has its own behavior of decomposition and reaction rate [40]. The three stages of coconut shells degradation can be identified by the TGA curve (Fig. 6). A temperature up to 300 °C is the dehydration stage for coconut shell. In this region, poorly bound water atoms and degradation of certain extractives occurred, as illustrated by the slope in Fig. 6. The process of dehydration resulted in a reduction of mass by 2.5 wt%. In the second region of the process, the devolatilization stage was identified as the stage with the highest mass loss. This region is commonly denoted to as the active pyrolysis region. The rate of decomposition in devolatilization stage was 18.8 wt% during pyrolysis. Throughout the devolatilization region of the pyrolysis process, the breakdown of cellulose, hemicellulose, and small volume of lignin occurred, leading to resulting in volatiles formation [41]. Larger molecular mass products are degraded into lower molecular mass products under steady non-isothermal thermal input [29].

The peak observed on the DTG curve in Fig. 5 represents the breakdown of natural polymer such as hemicellulose and cellulose [42]. Following the devolatilization stage, the substance that remained is regarded as biochar. The temperature up to 655 °C is the char formation stage for coconut shell. The process of combustion resulted in a reduction of mass by 14.2 wt% due to organic constituents burnt and volatized. It is known as the passive pyrolysis area, and it is at this stage that lignin is mostly degraded. The quantity of unburned material remaining after processing was 64.2 wt%. The pyrolysis process exhibited the maximum mass loss at 455 °C deducing from the DTG results. Mansaray and Ghaly [43] stated that this peak in mass loss can be explained as due to the decomposition of cellulose and hemicellulose, as well as the partial degradation of lignin. During the passive pyrolysis region, it was determined that the breakdown of lignin occurred at a much slower rate compared to other regions of the pyrolysis process.

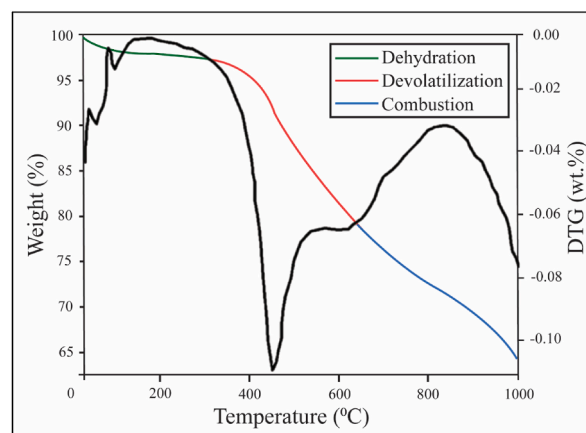


Fig. 5. TGA and DTG curve for coconut shells.

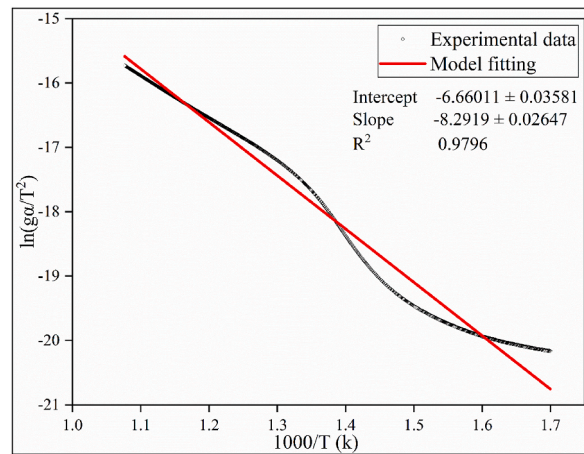


Fig. 6. DM6 (diffusion model) at 5 °C/min heating rate.

3.3. Kinetic analysis

The study focused on the estimation of the kinetics within the active pyrolysis range, where a one-step mechanism was assumed. A total of 21 reaction mechanisms categorized into 4 types, along with their respective kinetic parameters (E_a KJ.mol⁻¹ and A, min⁻¹). To identify the most suitable model, linear regression coefficient (R^2) was applied. The Coats-Redfern approach was selected to evaluate the kinetics of coconut shells. E_a (KJ.mol⁻¹) and A (min⁻¹) were analyzed using this method. The devolatilization region was selected for the kinetic analysis (315 °C–655 °C).

Table 3 shows the kinetic analysis for the devolatilization zone. Using 21 different reaction models, E_a , A, and R^2 values were calculated. Model CRO1, CRO2, CRO3, DM1, DM4, DM5, DM6, DM7, DM8, GM2 showed good regression coefficient ($R^2 = 0.96$ – 0.98) and this result agreed with the literature [44]. For 5 °C/min heating rate, the E_a of CRO1 model was 26.3 kJ mol⁻¹. The E_a for CRO1 and CRO1 are 32.6 kJ mol⁻¹ and 39.8 kJ mol⁻¹, respectively. The E_a for diffusion model DM6 was 68.9371938 kJ mol⁻¹ which showed the best regression coefficient ($R^2 = 0.98$). Diffusion models DM1, DM4, DM5, DM7 and DM8 also showed good regression coefficient with the E_a of 53.9 ± 3.66189 , 57.291774 ± 3.66189 , 58.5413682 ± 3.66189 , 61.0472078 ± 3.66189 , and 58.5280658 ± 3.66189 in KJ.mol⁻¹, respectively. GM2 represented a good regression coefficient ($R^2 = 0.962$) with the E_a of 24.3882876 ± 3.66189 kJ mol⁻¹.

The frequency factor exhibits a positive correlation with the heating rate across all reaction mechanism models. The frequency factor serves as an indicator of the collision frequency among the molecules undergoing reaction at a standard concentration. Bala-

Table 3
Kinetic parameters of devolatilization region.

Model	Devolatilization region		
	E_a (KJ.mol ⁻¹)	R^2	A (min ⁻¹)
CRO0	20.8041222	0.946	0.00015311
CRO1	26.3154728	0.967	0.00056746
CRO1.5	18.3481666	0.928	0.00025002
CRO2	32.6415954	0.974	0.00239729
CRO3	39.7592108	0.974	0.01150514
DM1	53.8797084	0.969	0.01985402
DM2	3.7429628	0.877	2.97E-06
DM3	13.4528834	0.944	5.50E-05
DM4	57.291774	0.973	0.0206045
DM5	58.5413682	0.974	0.00596844
DM6	68.9371938	0.98	0.0529606
DM7	61.0472078	0.976	0.01014418
DM8	58.5280658	0.974	0.0059225
GM1	23.457951	0.958	0.00014507
GM2	24.3882876	0.962	0.00012044
NM1	4.2667448	0.721	4.44E-06
NM2	0.1499	0.299	8.11E-08
NM3	4.0023596	0.87	1.56E-06
NM4	7.0220044	0.887	1.25E-05
NM5	0.5911254	0.103	4.58E-07
NM6	13.4528834	0.944	5.50E-05

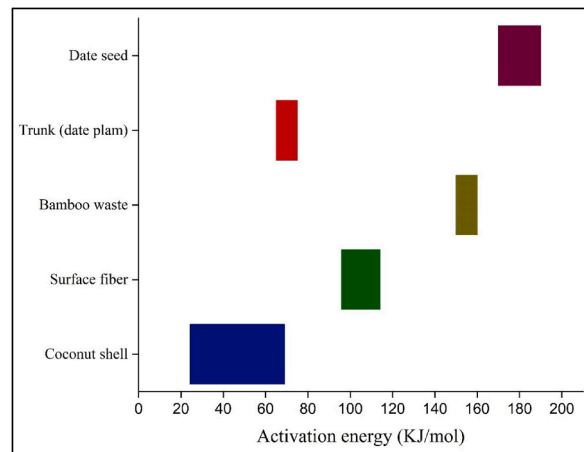


Fig. 7. Kinetic characteristics of several biomass resources.

Table 4

Thermodynamic characteristics of coconut shell pyrolysis.

Model	ΔH	ΔG	ΔS
CRO0	17.0212522	167.067428	-0.32977
CRO1	22.5326028	167.6231873	-0.31888
CRO1.5	14.5652966	162.7564275	-0.32569
CRO2	28.8587254	168.4984587	-0.3069
CRO3	35.9763408	169.6828161	-0.29386
DM1	50.0968384	181.7393329	-0.28932
DM2	-0.0399072	164.9155894	-0.36254
DM3	9.6700134	163.5896823	-0.33828
DM4	53.508904	185.0110423	-0.28902
DM5	54.7584982	190.9477012	-0.29932
DM6	65.1543238	193.085286	-0.28117
DM7	57.2643378	191.4470539	-0.29491
DM8	54.7451958	190.9636294	-0.29938
GM1	19.675081	169.9253057	-0.33022
GM2	20.6054176	171.5596578	-0.33177
NM1	0.4838748	163.9263191	-0.35921
NM2	-3.63297	174.9471503	-0.39248
NM3	0.2194896	167.6073556	-0.36789
NM4	3.2391344	162.7655615	-0.35061
NM5	-3.1917446	168.8400055	-0.37809
NM6	9.6700134	163.5896823	-0.33828

sundram, Ibrahim, Kasmani, Hamid, Isha, Hasbullah and Ali [45] suggested that the frequency factor is linked to the number of collisions between particles that take place in the proper orientation required for a successful reaction to occur.

In the devolatilization region, the Zhuravlev equation is found to be the best-fitted diffusion model, with the E_a of 68.9 kJ mol⁻¹. Fig. 6 shows the best fitting diffusion model. Fig. 7 shows the comparison of the E_a of different biomass sources. The approach of selecting an appropriate model for estimating kinetic parameters solely based on the highest regression coefficient (R^2) has been previously utilized by many researchers [46] for date seeds [47], for trunk (date palm) [48] for surface fiber using Coats-Redfern method, and [49] for bamboo waste using Ozawa-Wall-Flynn, Kissenger-Akahira- Sunose, and Friedman method.

3.4. Calculation of thermodynamic parameters

Table 4 represents the thermodynamic characteristics of coconut shell pyrolysis. Several kinds of reaction mechanisms were applied to identify the thermodynamic characteristics change in Gibbs free energy (ΔG); change in enthalpy (ΔH); change in entropy (ΔS). Thermodynamic characteristics were analyzed at a constant heating rate of 5 °C/min. Positive ΔH values indicate that coconut shells need external energy to initiate pyrolysis kinetics. The best-fitted model DM6 showed the enthalpy of 65.2 kJ mol⁻¹ ΔG gives information linked to the spontaneity of the reaction [50]. All ΔG values for each model are positive, suggesting that the decomposition of the coconut shell is not a spontaneous process. The best-fitted model DM6 showed the Gibbs free energy of 193.1 kJ mol⁻¹.

The calculated ΔS data are found to be negative, representing that the disorder of the products after dissociation is lower than that of the initial reactants. This suggests that the activated state during the thermal decay process has a more ordered structure associated to the initial reactants, and the reactions taking place in this state are more accessible than predicted. The best-fitted model DM6 showed the enthalpy of -0.28117 kJ mol⁻¹.

4. Conclusion

Coconut shell biomass holds significant promise as a renewable energy source for power generation. Our research reaffirmed the samples' potential for bioenergy, highlighted by their rough, fibrous surfaces and notable carbon content (56.1%), primarily constituted of lignocelluloses with an amorphous structure. Thermal and kinetic evaluations, using the Coats-Redfern method at a 5 °C/min heating rate, revealed a complex, multi-stage decomposition. The Zhuravlev diffusion equation (DM6) emerged as the most fitting model for this process, boasting an activation energy (E_a) of 68.9 kJ mol⁻¹ and a commendable R² value of 0.98. Thermodynamic metrics suggest that the sample's pyrolysis kinetics are endothermic and non-spontaneous, as inferred from ΔH and ΔG values. For enhanced yields in the devolatilization phase, we recommend investigating synergistic interactions between coconut shells and other organic fuels. While this study focused on a singular heating rate, future research should delve into varied rates, gauging their potential benefits for materials like coconut shells.

CRedit authorship contribution statement

Minhaj Uddin Monir: Conceptualization, Writing – original draft, Writing – review & editing. **Shaik Muntasir Shovon:** Data curation, Writing – original draft. **Faysal Ahamed Akash:** Software, Writing – original draft, Writing – review & editing. **Md Ahasan Habib:** Data curation, Writing – review & editing. **Kuaanan Techato:** Supervision, Funding acquisition, Investigation. **Azrina Abd Aziz:** Project administration, Supervision. **Shahariar Chowdhury:** Supervision, Writing – review & editing. **Tofan Agung Eka Prasetya:** Funding acquisition, Project administration, Writing – review & editing.

Declaration of competing interest

The authors declare that they have no known competing financial interests or personal relationships that could have appeared to influence the work reported in this paper.

Data availability

No data was used for the research described in the article.

Acknowledgements

The authors would like to express their sincere gratitude to Universitas Airlangga for providing the research opportunity. The authors would also like to thank the Energy Conversion Laboratory, Department of Petroleum and Mining Engineering, Jashore University of Science and Technology, Bangladesh and Universiti Malaysia Pahang, Malaysia for providing lab facilities.

References

- [1] J.L. Holeczek, H.M.E. Geli, M.N. Sawalhah, R. Valdez, A. Global Assessment, Can renewable energy replace fossil fuels by 2050? *Sustainability* 14 (8) (2022) 4792, <https://doi.org/10.3390/su14084792>.
- [2] D. Welsby, J. Price, S. Pye, P. Ekins, Unextractable fossil fuels in a 1.5 degrees C world (vol 597, pg 230, 2021), *Nature* 602 (7896) (2022) E22–E23, <https://doi.org/10.1038/s41586-021-03821-8>.
- [3] M.Y. Hasan, M.U. Monir, M.T. Ahmed, A.A. Aziz, S.M. Shovon, F. Ahamed Akash, M.F. Hossain Khan, M.J. Faruque, M.S. Islam Rifat, M.J. Hossain, P. Kundu, R. Akter, S. Ali, Sustainable energy sources in Bangladesh: a review on present and future prospect, *Renewable Sustainable Energy Rev.* 155 (2022) 111870, <https://doi.org/10.1016/j.rser.2021.111870>.
- [4] C. Bertram, G. Luderer, F. Creutzig, N. Bauer, F. Ueckerdt, A. Malik, O. Edenhofer, COVID-19-induced low power demand and market forces starkly reduce CO2 emissions, *Nat. Clim. Change* 11 (3) (2021) 193–196, <https://doi.org/10.1038/s41558-021-00987-x>.
- [5] M.A. Aktar, M.M. Alam, A.Q. Al-Amin, Global economic crisis, energy use, CO2 emissions, and policy roadmap amid COVID-19, *Sustain. Prod. Consum.* 26 (2021) 770–781, <https://doi.org/10.1016/j.spc.2020.12.029>.
- [6] J. Hu, Q. Tang, Z. Wu, B. Zhang, C. He, Q. Chen, Optimization and assessment method for total energy system retrofit in the petrochemical industry considering clean energy substitution for fossil fuel, *Energy Convers. Manag.* 284 (2023) 116967, <https://doi.org/10.1016/j.enconman.2023.116967>.
- [7] C. Wang, L. Zhang, P. Zhou, Y. Chang, D. Zhou, M. Pang, H. Yin, Assessing the environmental externalities for biomass- and coal-fired electricity generation in China: a supply chain perspective, *J. Environ. Manag.* 246 (2019) 758–767, <https://doi.org/10.1016/j.jenvman.2019.06.047>.
- [8] O. Kanat, Z. Yan, M.M. Asghar, Z. Ahmed, H. Mahmood, D. Kirikkaleli, M. Murshed, Do natural gas, oil, and coal consumption ameliorate environmental quality? Empirical evidence from Russia, *Environ. Sci. Pollut. Control Ser.* 29 (3) (2022) 4540–4556, <https://doi.org/10.1007/s11356-021-15989-7>.
- [9] Q. Li, The view of technological innovation in coal industry under the vision of carbon neutralization, *Int. J. Coal Sci. Technol.* 8 (6) (2021) 1197–1207, <https://doi.org/10.1007/s40789-021-00458-w>.
- [10] V. Tzelepi, M. Zeneli, D.-S. Kourkoumpas, E. Karampinis, A. Gypakis, N. Nikolopoulos, P. Grammelis, Biomass availability in Europe as an alternative fuel for full conversion of lignite power plants: a critical review, *Energies* 13 (13) (2020) 3390, <https://doi.org/10.3390/en13133390>.
- [11] J.M. Pedraza, *Conventional Energy in North America: Current and Future Sources for Electricity Generation*, Elsevier, 2019.
- [12] M.M. Vanegas Cantarero, Of renewable energy, energy democracy, and sustainable development: a roadmap to accelerate the energy transition in developing countries, *Energy Res. Social Sci.* 70 (2020) 101716, <https://doi.org/10.1016/j.erss.2020.101716>.
- [13] L. Li, J. Lin, N. Wu, S. Xie, C. Meng, Y. Zheng, X. Wang, Y. Zhao, Review and outlook on the international renewable energy development, *Energy Built Environ.* 3 (2) (2022) 139–157, <https://doi.org/10.1016/j.enbenv.2020.12.002>.
- [14] B. Yu, D. Fang, H. Yu, C. Zhao, Temporal-spatial determinants of renewable energy penetration in electricity production: evidence from EU countries, *Renew. Energy* 180 (2021) 438–451, <https://doi.org/10.1016/j.renene.2021.08.079>.
- [15] I. Ali, H. Bahaitham, R. Naebulharam, A comprehensive kinetics study of coconut shell waste pyrolysis, *Bioresour. Technol.* 235 (2017) 1–11, <https://doi.org/10.1016/j.biortech.2017.03.089>.
- [16] C. Cheng, L. Ding, Q. Guo, Q. He, Y. Gong, K.N. Alexander, G. Yu, Process analysis and kinetic modeling of coconut shell hydrothermal carbonization, *Appl. Energy* 315 (2022) 118981, <https://doi.org/10.1016/j.apenergy.2022.118981>.
- [17] J.C.G. da Silva, J.L.F. Alves, W.V. de Araujo Galdino, R.F. de Sena, S.L.F. Andersen, Pyrolysis kinetics and physicochemical characteristics of skin, husk, and shell from green coconut wastes, *Energy, Ecol. Environ.* 4 (3) (2019) 125–132, <https://doi.org/10.1007/s40974-019-00120-x>.
- [18] S. Thanigaivel, A.K. Priya, K. Dutta, S. Rajendran, K. Sekar, A.A. Jalil, M. Soto-Moscoso, Role of nanotechnology for the conversion of lignocellulosic biomass

- into biopotent energy: a biorefinery approach for waste to value-added products, *Fuel* 322 (2022) 124236, <https://doi.org/10.1016/j.fuel.2022.124236>.
- [19] M.U. Monir, A.A. Azrina, R.A. Kristanti, A. Yousuf, Gasification of lignocellulosic biomass to produce syngas in a 50 kW downdraft reactor, *Biomass Bioenergy* 119 (2018) 335–345, <https://doi.org/10.1016/j.biombioe.2018.10.006>.
- [20] Z. Fang, Y. Gao, N. Bolan, S.M. Shaheen, S. Xu, X. Wu, X. Xu, H. Hu, J. Lin, F. Zhang, Conversion of biological solid waste to graphene-containing biochar for water remediation: a critical review, *Chem. Eng. J.* 390 (2020) 124611, <https://doi.org/10.1016/j.cej.2020.124611>.
- [21] S. Chelouche, D. Trache, A.F. Tarchoun, A. Abdelaziz, K. Khimeche, A. Mezroua, Organic eutectic mixture as efficient stabilizer for nitrocellulose: kinetic modeling and stability assessment, *Thermochim. Acta* 673 (2019) 78–91, <https://doi.org/10.1016/j.tca.2019.01.015>.
- [22] I. Ali, S.R. Naqvi, A. Bahadar, Kinetic analysis of *Botryococcus braunii* pyrolysis using model-free and model fitting methods, *Fuel* 214 (2018) 369–380, <https://doi.org/10.1016/j.fuel.2017.11.046>.
- [23] S.R. Naqvi, Z. Hameed, R. Tariq, S.A. Taqvi, I. Ali, M.B.K. Niazi, T. Noor, A. Hussain, N. Iqbal, M. Shahbaz, Synergistic effect on co-pyrolysis of rice husk and sewage sludge by thermal behavior, kinetics, thermodynamic parameters and artificial neural network, *Waste Manage. (Tucson, Ariz.)* 85 (2019) 131–140, <https://doi.org/10.1016/j.wasman.2018.12.031>.
- [24] G. Rovelli, M.I. Jacobs, M.D. Willis, R.J. Rapf, A.M. Prophet, K.R. Wilson, A critical analysis of electrospray techniques for the determination of accelerated rates and mechanisms of chemical reactions in droplets, *Chem. Sci.* 11 (48) (2020) 13026–13043, <https://doi.org/10.1039/D0SC04611F>.
- [25] S. Vyazovkin, A.K. Burnham, J.M. Criado, L.A. Pérez-Maqueada, C. Popescu, N. Sbirrazzuoli, ICTAC Kinetics Committee recommendations for performing kinetic computations on thermal analysis data, *Thermochim. Acta* 520 (1) (2011) 1–19, <https://doi.org/10.1016/j.tca.2011.03.034>.
- [26] S.A. Akhade, N.J. Bernstein, M.R. Esopi, M.J. Regula, M.J. Janik, A simple method to approximate electrode potential-dependent activation energies using density functional theory, *Catal. Today* 288 (2017) 63–73, <https://doi.org/10.1016/j.cattod.2017.01.050>.
- [27] V. Dhyani, J. Kumar, T. Bhaskar, Thermal decomposition kinetics of sorghum straw via thermogravimetric analysis, *Bioresour. Technol.* 245 (2017) 1122–1129, <https://doi.org/10.1016/j.biortech.2017.08.189>.
- [28] A.W. Coats, J.P. Redfern, Kinetic parameters from thermogravimetric data, *Nature* 201 (4914) (1964) 68–69, <https://doi.org/10.1038/201068a0>.
- [29] R.K. Mishra, K. Mohanty, Pyrolysis kinetics and thermal behavior of waste sawdust biomass using thermogravimetric analysis, *Bioresour. Technol.* 251 (2018) 63–74, <https://doi.org/10.1016/j.biortech.2017.12.029>.
- [30] M.S. Ahmad, M.A. Mehmood, O.S. Al Aayed, G. Ye, H. Luo, M. Ibrahim, U. Rashid, I. Arbi Nehdi, G. Qadir, Kinetic analyses and pyrolytic behavior of Para grass (*Urochloa mutica*) for its bioenergy potential, *Bioresour. Technol.* 224 (2017) 708–713, <https://doi.org/10.1016/j.biortech.2016.10.090>.
- [31] Z. Zhang, Z. Zhu, B. Shen, L. Liu, Insights into biochar and hydrochar production and applications: a review, *Energy* 171 (2019) 581–598, <https://doi.org/10.1016/j.energy.2019.01.035>.
- [32] S.D. Menon, K. Sampath, S.S. Kaarthik, Feasibility studies of coconut shells biomass for downdraft gasification, *Mater. Today: Proc.* 44 (2021) 3133–3137, <https://doi.org/10.1016/j.matpr.2021.02.813>.
- [33] A. Coppola, R. Solimene, P. Bareschino, P. Salatino, Mathematical modeling of a two-stage fuel reactor for chemical looping combustion with oxygen uncoupling of solid fuels, *Appl. Energy* 157 (2015) 449–461, <https://doi.org/10.1016/j.apenergy.2015.04.052>.
- [34] G. Montero, M.A. Coronado, R. Torres, B.E. Jaramillo, C. García, M. Stoytcheva, A.M. Vázquez, J.A. León, A.A. Lambert, E. Valenzuela, Higher heating value determination of wheat straw from Baja California, Mexico, *Energy* 109 (2016) 612–619, <https://doi.org/10.1016/j.energy.2016.05.011>.
- [35] A. Zubair Yahaya, M. Rao Somalu, A. Mughtar, S. Anwar Sulaiman, W. Ramli Wan Daud, Effects of temperature on the chemical composition of tars produced from the gasification of coconut and palm kernel shells using downdraft fixed-bed reactor, *Fuel* 265 (2020) 116910, <https://doi.org/10.1016/j.fuel.2019.116910>.
- [36] Q. Yu, J.M. Bowman, Tracking hydronium/water stretches in magic H₃O⁺ (H₂O) 20 clusters through high-level quantum VSCF/VCI calculations, *J. Phys. Chem.* 124 (6) (2020) 1167–1175, <https://doi.org/10.1021/acs.jpca.9b11983>.
- [37] H. Bi, Z. Ni, J. Tian, C. Wang, C. Jiang, W. Zhou, L. Bao, H. Sun, Q. Lin, The effect of biomass addition on pyrolysis characteristics and gas emission of coal gangue by multi-component reaction model and TG-FTIR-MS, *Sci. Total Environ.* 798 (2021) 149290, <https://doi.org/10.1016/j.scitotenv.2021.149290>.
- [38] C.-F. Liu, J.-L. Ren, F. Xu, J.-J. Liu, J.-X. Sun, R.-C. Sun, Isolation and characterization of cellulose obtained from ultrasonic irradiated sugarcane bagasse, *J. Agric. Food Chem.* 54 (16) (2006) 5742–5748, <https://doi.org/10.1021/jf060929o>.
- [39] V. Nang An, H.T. Chi Nhan, T.D. Tap, T.T.T. Van, P. Van Viet, L. Van Hieu, Extraction of high crystalline nanocellulose from biorenewable sources of Vietnamese agricultural wastes, *J. Polym. Environ.* 28 (5) (2020) 1465–1474, <https://doi.org/10.1007/s10924-020-01695-x>.
- [40] R. Kaur, P. Gera, M.K. Jha, T. Bhaskar, Pyrolysis kinetics and thermodynamic parameters of castor (*Ricinus communis*) residue using thermogravimetric analysis, *Bioresour. Technol.* 250 (2018) 422–428, <https://doi.org/10.1016/j.biortech.2017.11.077>.
- [41] Ö. Çepelioğullar, A.E. Pütün, Thermal and kinetic behaviors of biomass and plastic wastes in co-pyrolysis, *Energy Convers. Manag.* 75 (2013) 263–270, <https://doi.org/10.1016/j.enconman.2013.06.036>.
- [42] H. Fan, J. Gu, Y. Wang, H. Yuan, Y. Chen, Kinetics modeling of co-pyrolytic decomposition of binary system of cellulose, xylan and lignin, *J. Energy Inst.* 102 (2022) 278–288, <https://doi.org/10.1016/j.joei.2022.03.012>.
- [43] K.G. Mansaray, A.E. Ghalay, Thermal degradation of rice husks in nitrogen atmosphere, *Bioresour. Technol.* 65 (1) (1998) 13–20, [https://doi.org/10.1016/S0960-8524\(98\)00031-5](https://doi.org/10.1016/S0960-8524(98)00031-5).
- [44] A. Inayat, F. Jamil, S.F. Ahmed, M. Ayoub, P.M. Abdul, M. Aslam, M. Mofijur, Z. Khan, A. Mustafa, Thermal degradation characteristics, kinetic and thermodynamic analyses of date palm surface fibers at different heating rates, *Fuel* 335 (2023) 127076, <https://doi.org/10.1016/j.fuel.2022.127076>.
- [45] V. Balasundram, N. Ibrahim, R.M. Kasmani, M.K.A. Hamid, R. Isha, H. Hasbullah, R.R. Ali, Thermogravimetric catalytic pyrolysis and kinetic studies of coconut copra and rice husk for possible maximum production of pyrolysis oil, *J. Clean. Prod.* 167 (2017) 218–228, <https://doi.org/10.1016/j.jclepro.2017.08.173>.
- [46] M. Raza, B. Abu-Jdayil, A. Inayat, Pyrolytic kinetics and thermodynamic analyses of date seeds at different heating rates using the Coats–Redfern method, *Fuel* 342 (2023) 127799, <https://doi.org/10.1016/j.fuel.2023.127799>.
- [47] M. Jeguirim, Y. Elmay, L. Limousy, M. Lajili, R. Said, Devolatilization behavior and pyrolysis kinetics of potential Tunisian biomass fuels, *Environ. Prog. Sustain. Energy* 33 (4) (2014) 1452–1458, <https://doi.org/10.1002/ep.11928>.
- [48] M. Raza, B. Abu-Jdayil, A.H. Al-Marzouqi, A. Inayat, Kinetic and thermodynamic analyses of date palm surface fibers pyrolysis using Coats-Redfern method, *Renew. Energy* 183 (2022) 67–77, <https://doi.org/10.1016/j.renene.2021.10.065>.
- [49] Z. Liu, A. Asghar, C. Hou, I. Ali, S.R. Naqvi, N. Wang, H. Zhu, M.A. Mehmood, C.-G. Liu, Co-pyrolysis of the Chinese liquor industry waste and bamboo waste, elucidation of the pyrolysis reaction chemistry, and TG-FTIR-MS based study of the evolved gases, *Fuel* 326 (2022) 124976, <https://doi.org/10.1016/j.fuel.2022.124976>.
- [50] J.G.O. Marques, A.L. Costa, C. Pereira, Gibbs free energy (ΔG) analysis for the NaOH (sodium-oxygen-hydrogen) thermochemical water splitting cycle, *Int. J. Hydrogen Energy* 44 (29) (2019) 14536–14549, <https://doi.org/10.1016/j.ijhydene.2019.04.064>.